

# QUANTUM THERMODYNAMICS AT THE CRITICAL POINTS DURING MELTING AND SOLIDIFICATION PROCESSES

ANDREW DAS ARULSAMY

**ABSTRACT.** Phase transitions are ubiquitous, exist in all fields of science in one form or another. The most common example in condensed matter physics is the thermal phase transition from a liquid to solid phase. Here, we systematically explore and develop unequivocal theoretical strategies, going beyond the total-energy minimization techniques to understand what constitutes the finite-temperature continuous quantum phase transitions ( ${}^C_T$ QPT). In fact, this  ${}^C_T$ QPT is actually related to the qualitative discussion given by Sachdev, whom is the first to point out the existence of a QPT in ice for different pressures at the freezing point. To extract the quantitative information related to  ${}^C_T$ QPT, we first exploit the energy level spacing renormalization group method to renormalize (i) the electronic-excitation and atomic-disorder (or symmetry-breaking) entropies, (ii) the specific heat capacity and (iii) the Bose-Einstein distribution. Subsequently, we prove the existence of the  ${}^C_T$ QPT in the solid to liquid phase transition, and further develop the necessary proof for the existence of a non-divergent time-dependent specific heat at the critical point of a first-order thermal phase transition.

PACS: 05.30.Rt; 05.30.Fk; 05.70.Jk; 05.70.Ln  
MSC: 82C26; 82C27; 82C22

## 1. INTRODUCTION

Unlike any thermal fluctuation, the fluctuation at a critical point of a finite-temperature continuous quantum phase transition ( ${}^C_T$ QPT) is specifically called quantum fluctuation (even for finite temperatures) because it is related to the properties of electrons at a constant temperature, and therefore, it is still subject to the established Heisenberg uncertainty principle. An example in this respect is the existence of a  ${}^C_T$ QPT (due to changing pressure), which is well-known for ice at a constant temperature ( $0 < T < 273.16\text{K}$ ). The readers are referred to an elementary and straightforward discussion on these two issues (quantum fluctuation and  ${}^C_T$ QPT in ice) given by Sachdev [1].

This  ${}^C_T$ QPT gives rise to the existence of finite temperature quantum critical points ( ${}^T$ QCP), such that the quantum fluctuation with an energy scale,  $\hbar\omega$  can be written as,

$$(1.1) \quad \hbar\omega(y_1) < k_B T_\theta,$$

$$(1.2) \quad \hbar\omega(y_2) = k_B T_\theta,$$

$$(1.3) \quad \hbar\omega(y_3) > k_B T_\theta,$$

---

*Date:* January 23, 2023.

*Key words and phrases.* Thermal and quantum phase transitions; Energy-level spacing and time-dependent entropy; Ionization energy theory; Energy-level spacing renormalization method.

where  $\hbar$  is the Planck constant divided by  $2\pi$ ,  $k_B$  denotes the Boltzmann constant,  $\omega(y)$  and  $T_\theta$  are the doping ( $y$ )-dependent frequency and some critical temperature (a  $T$ QCP), respectively. For  $0K$ QCP, the relevant inequality is simply  $\hbar\omega(y_1) < \hbar\omega(y_2) < \hbar\omega(y_3)$  because  $T_\theta = 0K$ . Here,  $y_1$ ,  $y_2$  and  $y_3$  are related to different chemical composition, while  $\theta$  represents a certain physical property under investigation. For example, for the melting process (chemical dissociation),  $T_\theta = T_{\text{point}}^{\text{melting}}$ , and it satisfies the classical phase transition (due to thermal fluctuation with increasing temperature for a given chemical composition), without any microscopic understanding as to the reasons why and how the translational symmetry breaks (ice to water). This does not imply melting is a classical process not involving electrons. For instance, we have proven how the energy level spacing evolve and give rise to a changing interaction strength between a polarizable water molecule physisorbed onto the MgO surface, which then initiate the water molecule dissociation at a constant temperature [2]. Within the ionization energy theory (IET) [3, 4, 5], we can write  $\hbar\omega(y) = \xi(y)$  where  $\xi(y)$  is the ionization energy of a particular compound, and it is also known as the energy level spacing within the renormalization group method [6]. Hence, during chemical dissociation with changing chemical composition,  $\xi(y)$  is a dynamical parameter, giving rise to quantum fluctuation. Importantly, much below the melting point, fluctuation in  $\xi(y)$  is caused by the energy level crossings, changes in the valence states of the constituent elements, and defects due to different chemical compositions (doping) along a constant temperature line. Such fluctuations (due to defects and valence states) are responsible for the changes in the constant-temperature and composition-dependent (i) resistivity of ferromagnets [7] and in the normal-state of superconductors [3, 8, 9], (ii) non-blinking effect in quantum dots [10] and (iii) reversible carrier-type transition in oxides [11].

In the subsequent section, we introduce the first-order thermal phase transition before venturing deeper into the details of quantum phase transition and quantum fluctuation. Along the way, the theory is discussed and crosschecked whenever necessary against the experimental observations. Finally, we will conclude that (a) the finite-temperature continuous quantum phase transition is responsible for the first-order thermal phase transition, and (b) at the critical point of a first-order thermal phase transition, a non-divergent time-dependent specific heat can be proven to exist. For the recent experimental and theoretical developments of the zero temperature quantum phase transitions in strongly interacting solids, we refer the readers to Refs. [12, 13, 14, 15, 16, 17, 18, 19, 20, 21, 22, 23, 24, 25].

## 2. FURTHER ANALYSES ON THE THERMAL AND QUANTUM FLUCTUATIONS

Here, we will give rigorous and unambiguous logical proofs (supported by experimental results, of course) on the origin of thermal and quantum fluctuations due to temperature and doping (or  $\xi(y)$ ) within IET. But before doing so, we need to justify the reasons why we have selected salts made up of single-valent cations and anions from group 17 of the periodic table as listed in Table 1.

Table 1 lists the diatomic bonding energies and melting points of these salts such that the melting points decrease systematically with decreasing bonding energies from F to I. Such a decreasing trend can be precisely overlapped with the decreasing ionization energies of the anions, namely,  $\xi_{F^-} (1681 \text{ kJmol}^{-1}) > \xi_{Cl^-} (1251$

TABLE 1. Experimental values for the melting points and diatomic bonding energies of salts obtained from Refs. [26] and [27], respectively. The systematic decrease of the melting points and diatomic bonding energies with respect to anions (from F to I with increasing  $Z$ ) satisfy the decreasing ionization energies for the same anions, from F to I. See the text and Table 2 (follow the values marked with “ \* ”) for details.

| Salts | Melting points<br>(°C) | Diatomic bonding<br>energies (kJmol <sup>-1</sup> ) |
|-------|------------------------|---|
| LiF   | 848                    | 577   |
| LiCl  | 610                    | 469   |
| LiBr  | 552                    | 419   |
| LiI   | 469                    | 345   |
| NaF   | 996                    | 519   |
| NaCl  | 801                    | 412   |
| NaBr  | 747                    | 367   |
| NaI   | 660                    | 304   |
| KF    | 858                    | 498   |
| KCl   | 771                    | 433   |
| KBr   | 734                    | 380   |
| KI    | 681                    | 325   |
| RbF   | 833                    | 494   |
| RbCl  | 715                    | 428   |
| RbBr  | 682                    | 381   |
| RbI   | 642                    | 319   |

kJmol<sup>-1</sup>) >  $\xi_{\text{Br}^+}$ (1140 kJmol<sup>-1</sup>) >  $\xi_{\text{I}^+}$ (1008 kJmol<sup>-1</sup>). The values in the inequalities are given in Table 2, follow the values marked with “ \* ”. Interestingly however, for a given anion, the decreasing melting points do not agree with the ionization energy values of the cations: Li, Na, K and Rb (follow their values listed in Table 2, marked with “ † ”). For example, the melting points for NaF (996°C) > KF (858°C) > LiF (848°C) > RbF (833°C) cannot be overlapped with  $\xi_{\text{Li}^+}$ (520 kJmol<sup>-1</sup>) >  $\xi_{\text{Na}^+}$ (496 kJmol<sup>-1</sup>) >  $\xi_{\text{K}^+}$ (419 kJmol<sup>-1</sup>) >  $\xi_{\text{Rb}^+}$ (403 kJmol<sup>-1</sup>). This is not surprising because melting is a process directly proportional to bonding strengths (see Table 1), which have been discussed earlier [11] within IET where large ionization energy values of cation-like ions ( $\xi_{\text{C}^{2+}} < \xi_{\text{O}^{2+}}$ ) in a given molecule ( $\text{C}^{2+}\text{O}^{2-}$  or  $\text{O}_{(1)}^{2-}\text{O}_{(2)}^{2+}$ ) do not necessarily imply stronger bonds. Fortunately, we have proven that a stronger bond is predictable from IET if one considers the ionization energies of anions (say O in H<sub>2</sub>O), because oxygen defines the ability to attract electrons from an atomic hydrogen [2]. In this case, smaller  $\xi_{\text{O}}$  means weaker O–H bond, which is consistent with the above-stated ionization-energy inequalities for anions (group 17 elements) and the melting points.

In Table 2, we have deliberately selected systems consisting of single valent cations and anions from group 17 to avoid effects from different electronic interactions due to different number (and type) of constituent atoms in a given molecule. To understand this point, we again use molecular systems, in which, for a NO<sub>2</sub> molecule, N acts as a cation, while O as an anion, which means that we need to

TABLE 2. Averaged atomic ionization energies ( $\xi$ ) for individual ions and their respective valence states ordered with increasing atomic number  $Z$ . All the experimental ionization energy values were obtained from Ref. [27].

| Elements | Atomic numbers<br>$Z$ | Valence<br>states | $\xi$<br>(kJmol <sup>-1</sup> ) |
|----------|-----------------------|-------------------|---------------------------------|
| H        | 1                     | 1+                | 1312                            |
| Li       | 3                     | 1+                | 520†                            |
| N        | 7                     | 1+                | 1402                            |
| N        | 7                     | 4+                | 4078                            |
| O        | 8                     | 1+                | 1314                            |
| O        | 8                     | 2+                | 2351                            |
| O        | 8                     | 4+                | 4368                            |
| F        | 9                     | 1+                | 1681*                           |
| Na       | 11                    | 1+                | 496†                            |
| Cl       | 17                    | 1+                | 1251*                           |
| K        | 19                    | 1+                | 419†                            |
| Br       | 35                    | 1+                | 1140*                           |
| Rb       | 37                    | 1+                | 403†                            |
| Sr       | 38                    | 2+                | 807                             |
| I        | 53                    | 1+                | 1008*                           |
| La       | 57                    | 3+                | 1152                            |

consider the valence state of 4+ since 4 electrons have been transferred from N<sup>4+</sup> to O<sub>2</sub><sup>2-</sup>. This electron-transfer is due to  $\xi_{N^{4+}} < \xi_{O^{4+}}$  (see Table 1). In contrast, N is an anion in NH<sub>3</sub> molecule due to  $\xi_{N^{+}} > \xi_{H^{+}}$  where 3 electrons from 3 hydrogen atoms are transferred to nitrogen, giving N<sup>3-</sup>H<sub>3</sub><sup>+</sup>. Thus far, the analyses are correct. However, the polarizability of the molecule NO<sub>2</sub> *does not* solely depend on these 4 electrons contributed by nitrogen if we compare N<sup>4+</sup>O<sub>2</sub><sup>2-</sup> with N<sup>3-</sup>H<sub>3</sub><sup>+</sup> because we cannot simplify the analysis by comparing  $\xi_{N^{4+}}$  with  $\xi_{H^{+}}$  (3 electrons contributed by 3 hydrogen ions) only. If we do so, then obviously we have  $\xi_{N^{4+}} > \xi_{H^{+}}$  that falsely allows us to conclude  $\alpha_d^{NO_2} < \alpha_d^{NH_3}$  because  $\alpha_d \propto \exp(-\xi)$  where  $\alpha_d$  is the displacement polarizability.

In other words, we cannot use the above inequality ( $\xi$ ) to directly compare  $\alpha_d$  between NO<sub>2</sub> and NH<sub>3</sub> molecules because N acts as a cation in a NO<sub>2</sub> molecule, while it is an anion for the molecule, NH<sub>3</sub>. This implies that we need to take both the cationic- and anionic-effect into account explicitly for an accurate logical analysis, which have been correctly invoked in Ref. [2]. However, the anionic-effect can be neglected when we compare CO with O<sub>2</sub> because in these molecules, oxygen is the anion and therefore  $\alpha_d^{CO} < \alpha_d^{O_2}$  is valid [11]. On the other hand, the justification required to neglect the cationic-effect for doped-Pnictide superconductors is given in Ref. [9]. Finally, taking both cationic- and anionic-effect into account means that for large (many-electron) cations such as K ( $Z = 19$ ) and Rb ( $Z = 37$ ), there will always be some significant amount of polarization (due to large screening) from the outer core electrons, even though effectively, K<sup>+</sup> and Rb<sup>+</sup> are single-valent ions. This second- or third-electron polarization is negligible for few-electron atoms (due to small screening), namely, Li ( $Z = 3$ ) and interestingly, also for Na ( $Z = 11$ ).

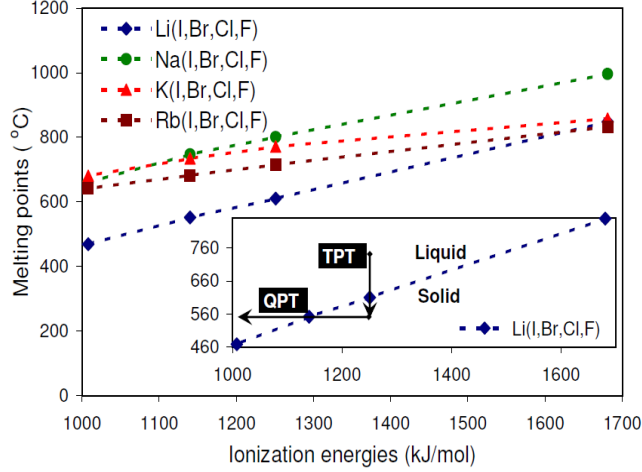


FIGURE 1. Melting points of Li(I,Br,Cl,F), Na(I,Br,Cl,F), K(I,Br,Cl,F) and Rb(I,Br,Cl,F) salts are plotted against the anionic (I,Br,Cl,F) ionization energies, which indicate a direct proportionality between them (follow the dotted lines). INSET: The vertical down-arrow (solidification) denotes a first-order thermal phase transition (from liquid to solid) for LiCl when the temperature is reduced from  $T > 610^\circ\text{C}$  to  $T = 552^\circ\text{C}$ . The horizontal arrow pointing left captures the continuous (purely electronic) quantum phase transition (from solid to liquid) at constant  $T = 552^\circ\text{C}$  by changing the chemical composition systematically,  $\text{LiCl}_{1-a_1}\text{Br}_{a_1-a_2}\text{I}_{a_2}$  such that  $\text{LiCl} \rightarrow \text{LiBr} \rightarrow \text{LiI}$ ,  $y_3 = 1 - a_1$ ,  $y_2 = a_1 - a_2$  and  $y_1 = a_2$ .

Note here that we need smaller and larger ionization energies for cations and anions, respectively for stronger ionic bonds. Therefore, incorporating this additional amount of polarization (for cations) implies larger  $\xi_{\text{cationic}}$  or equivalently, smaller  $\xi_{\text{anionic}}$  that should reduce the melting point as has been observed experimentally (see Fig. 1). Importantly, this correction does not apply for anions if a given system consists of mostly ionic bonds because the anions are judged solely on their ability to attract electrons from the cations. On the contrary, for systems with mostly covalent bonds, we need to consider both cationic- and anionic-effect simultaneously as carried out in Ref. [2]. The existence of this additional polarization is consistent with the experimental results shown in Fig. 1 when one compares the slope,  $dT_\theta/d\xi$  for salts containing Li and Na, for instance  $(dT_\theta/d\xi)_{\text{Li}} \approx (dT_\theta/d\xi)_{\text{Na}}$ , while  $(dT_\theta/d\xi)_{\text{K}} \approx (dT_\theta/d\xi)_{\text{Rb}}$  (follow the dotted lines in Fig. 1).

### 3. RENORMALIZED ENTROPY, SPECIFIC HEAT AND BOSE-EINSTEIN STATISTICS

Figure 1 shows the direct proportionality between melting points and ionization energies of the constituent anions (I,Br,Cl,F). The respective vertical and horizontal arrows in the inset of Fig. 1 indicate the first-order TPT and  $T$ -QPT. In order to expose the existence of these phase transitions, we need to recall the first and second

laws of thermodynamics. These two laws can be combined to obtain

$$(3.1) \quad dU = \delta Q + \delta W = TdS - PdV,$$

in which, the change in the internal energy,  $dU$  of a closed system equals the amount of heat ( $Q$ ) absorbed and the amount of work ( $W$ ) done by that system. Here,  $\delta$  is not an exact differential because the changes in  $Q$  and  $W$  depend on the thermodynamic path (or independent of a particular system and process), and therefore,  $Q$  and  $W$  are not state functions. Here,  $P$  and  $V$  denote pressure and volume, respectively and we consider only reversible processes. Unlike  $Q$  and  $W$ , the thermodynamic variable  $U$ ,  $P$  and  $V$  are state functions that are unique for a given system and process. The second law is given by,  $\delta Q = TdS$  where  $S$  is the entropy, another path-independent state function. All we need now is the relationship connecting  $S$  to  $\xi$  that can be obtained from the derivation of the ionization energy based Fermi-Dirac statistics (*iFDS*). Denoting  $N$  as the total number of particles with  $n_1$  particles have energy  $(E_0 \pm \xi)_1$ ,  $n_2$  particles with energy  $(E_0 \pm \xi)_2$  and so on implies that  $N = n_1 + n_2 + \dots + n_m$ . As a consequence, the number of ways for  $q_1$  unoccupied quantum states to be arranged among  $n_1$  particles is

$$(3.2) \quad \Omega(n_1, q_1) = \frac{q_1!}{n_1!(q_1 - n_1)!},$$

satisfying the condition that one empty quantum state can accommodate only one particle. Subsequently, the total number of ways for  $q$  quantum states ( $q = q_1 + \dots + q_m$ ) to be arranged among  $N$  particles

$$(3.3) \quad \Omega(N, q) = \prod_i \frac{q_i!}{n_i!(q_i - n_i)!}.$$

The most probable configuration for certain  $T$  can be obtained by maximizing the number of ways one can arrange  $n_i$  particles in  $q_i$  empty quantum states or, we need to maximize  $\Omega(N, q)$  subject to the restrictive conditions,

$$(3.4) \quad \sum_i n_i = N, \quad \sum_i dn_i = 0,$$

$$(3.5) \quad \sum_i (E_0 \pm \xi)_i = E, \quad \sum_i (E_0 \pm \xi)_i dn_i = 0.$$

These conditions impose that the total energy,  $E$  and the total number of particles,  $N$  for a given system are always constant. Here,  $E_0$  is the total energy for 0K. The method of Lagrange multipliers [28] can be employed to maximize Eq. (3.3) by first introducing a new function,  $F_{\text{new}}(\dots, \mu, \lambda, \dots) = \dots + \mu f_1 + \lambda f_2 + \dots$ , such that

$$(3.6) \quad F_{\text{new}} = \ln \Omega(N, q) + \mu \sum_i n_i + \lambda \sum_i (E_0 \pm \xi)_i n_i,$$

where  $n_1 = n_2 = n_3 \dots = n_i = 1$  to imply one empty quantum state ( $q$ ) or energy level can accommodate only one particle (either electron or hole). Subsequently (we maximize  $F_{\text{new}}$ ),

$$(3.7) \quad \frac{\partial F_{\text{new}}}{\partial n_i} = \frac{\partial [\ln \Omega(N, q)]}{\partial n_i} + \mu \sum_i \frac{\partial n_i}{\partial n_i} + \lambda \sum_i (E_0 \pm \xi)_i \frac{\partial n_i}{\partial n_i} = 0.$$

Equation (3.7) can be solved subject to the conditions,  $n_i \gg 1$ ,  $q_i \gg 1$ ,  $q_i \geq n_i$  that give us the license to use Stirling's approximation ( $\ln(n_i!) \approx n_i \ln n_i - n_i$ ), and after some algebraic rearrangements, one gets

$$(3.8) \quad \frac{N}{q} = \frac{1}{\exp[\mu + \lambda(E_0 \pm \xi)] + 1},$$

which is the *i*FDS. Taking  $\exp[\mu + \lambda(E_0 \pm \xi)] \gg 1$ ,  $\mu = -\lambda E_F^0$  and dividing all the terms by  $T$  will lead us to the energy-level spacing entropy

$$(3.9) \quad S_\xi = -\frac{(E_0 \pm \xi) + E_F^0}{T} = \frac{1}{(\lambda_B, \lambda)T} \ln \frac{N}{q},$$

in which,

$$(3.10) \quad \lambda_B = \frac{1}{k_B T} \text{ for constant } \xi \text{ and}$$

$$(3.11) \quad \lambda = \frac{12a_B \pi \epsilon_0}{e^2} \text{ for constant } T > 0.$$

The derivation for  $\lambda_B$  is well known in classical thermodynamics and is also given in Ref. [5] within the IET formalism, while the proof for  $\lambda$  is available in Ref. [4]. Here,  $E_F^0$  denotes the Fermi level for  $T = 0\text{K}$ , independent of any disturbance,  $a_B$  is the Bohr radius of atomic hydrogen,  $e$  and  $\epsilon_0$  denote the electron charge and the permittivity of free space, respectively. The entropy  $S_\xi$  given in Eq. (3.9) decreases logarithmically ( $S_\xi \rightarrow -\infty$ ) when  $N/q \rightarrow 0$  (ordered) such that, the inequality  $0 < N/q < 1$  strictly corresponds to  $-\infty_{\min} < S_\xi < 0_{\max}$ . Furthermore, within the set of real negative numbers, including zero ( $S_\xi \in \mathbb{R}^-$ ) and Eq. (3.9), we have the correct correspondence between  $T \rightarrow 0$  and  $S_\xi \rightarrow -\infty$  (ordered).

The other relevant entropy is due to atomic-disorder,  $S_D = k_B \ln D$  where

$$(3.12) \quad D(N_D, q_D) = \prod_i \frac{(n_i + q_i - 1)!}{n_i!(q_i - 1)!} \approx \prod_i \frac{(n_i + q_i)!}{n_i!q_i!},$$

by taking  $n_i \gg 1$ ,  $q_i \gg 1$  and defining  $N_D/q_D$  as the ratio of the total number of particles and empty quantum states. Here,  $N_D/q_D$  is proportional to the excited phonon density that will tell us the probability of ionic conductivity. One of the two restrictive conditions needed to maximize Eq. (3.12) remains the same (Eq. (3.4)), while the condition for the total energy has been renormalized,

$$(3.13) \quad \sum_i [E e^{\frac{1}{2}\lambda(\xi - E_F^0)}]_i n_i = \tilde{E}.$$

The explicit renormalization procedure follows Ref. [6]. This renormalized total energy takes the properties of the valence electrons into account to evaluate the phonon densities and the ionic hopping probability. Following the same procedure used to derive *i*FDS and taking  $E_F^0 = 0$  (because it is an irrelevant constant within IET), we obtain the renormalized Bose-Einstein statistics (*r*BES)

$$(3.14) \quad \frac{N_D}{q_D} = \frac{1}{\exp[\lambda_B E e^{\frac{1}{2}\lambda\xi}] - 1}.$$

It is important to note here that  $q_D \geq N_D$  is required so that the probability is normalized to one, even if there can be any number of  $n$  particles allowed to occupy a single empty quantum state,  $q$ . Similar to  $S_\xi$ ,  $S_D \in \mathbb{R}^-$ . We are now ready to track the solidification of liquid LiCl from  $T_2 > 610^\circ\text{C}$  to  $T_1 = 552^\circ\text{C}$  as shown in

the inset of Fig. 1. In this case, the dominant entropy change is due to the transition from the disordered (liquid state) to an ordered (solid) state in which, the liquid state is defined within  $610^\circ\text{C} < T \leq T_2$  and the solid state is bounded within  $T_1 \leq T < 610^\circ\text{C}$ . The value  $610^\circ\text{C}$  ( $T_\theta$ ) is the critical point, or the melting point of LiCl and  $S_D^{\text{liquid}} > S_D^{\text{solid}}$  indicates the existence of TPT, qualitatively that is. To claim liquid has a larger entropy than solid implies we have invoked an additional condition  $|S_D^{\text{liquid}} - S_D^{\text{solid}}| > |S_\xi^{\text{liquid}} - S_\xi^{\text{solid}}|$  because the change of entropy due to electronic excitation is always smaller compared to an atomic-disorder induced entropy (due to broken translational symmetry) within a particular system. Of course, in the absence of this temperature-induced atomic-arrangement asymmetry, electronic disorder or  $S_\xi$  is the dominant one.

Apparently, the change in the entropy during the above-stated transition (solidification) is a first-order TPT because  $S_{D:T>T_\theta}^{\text{liquid}} > S_{D:T<T_\theta}^{\text{solid}}$  such that there exist a nonequilibrium entropy ( $S_{\text{eq}}^{\text{non}}$ ) that contribute to this inequality, which is classically undefined at the critical point,  $T = T_\theta = 610^\circ\text{C}$  where both solid and liquid phases coexist. However, we can define  $S_{\text{eq}}^{\text{non}}$  with respect to the time-dependent energy-level spacing,  $\xi(t)$  and using Eq. (3.9) at the critical point due to time-dependent processes of breaking and forming of bonds [2, 30] at the solid|liquid interface (we will revisit this issue in detail shortly) for  $T = T_\theta$ . In this case,  $\xi$  continuously switches between  $\xi^{\text{liquid}}$  and  $\xi^{\text{solid}}$  for  $T = T_\theta$ . Consequently, one cannot write  $S_D^{\text{solid}} < S_{\text{eq}}^{\text{non}} < S_D^{\text{liquid}}$ , which in turn implies that solidification and melting are first-order transitions. Traditionally however, a first-order TPT is defined to exist if there is a quantitative discontinuity in the thermodynamic variable. For example, the heat capacity (a thermodynamic variable) is discontinuous at the critical point due to discontinuity in the entropy itself as stated above. Here, the constant-volume heat capacity and entropy relationship can be obtained from

$$(3.15) \quad dS = \frac{dU + PdV}{T} = \frac{1}{T} \left[ \left. \frac{\partial U}{\partial T} \right|_V + 0 \right] = \frac{C_v}{T} dT,$$

using Eq. (3.1) and the definition,  $C_v = \partial U / \partial T|_V$ , in which Eq. (3.15) tells us nothing about the changes in  $C_v$  during solidification or at the critical point, except that it diverges [29]. Anyway, on the way to understand the origin of the first order TPT (given above), we have pointed out the existence of time-dependent  $\xi(t)$ , which fluctuates between  $\xi^{\text{liquid}}$  and  $\xi^{\text{solid}}$  for  $T = T_\theta$  in the presence of both solid and liquid phases. Now, the above fluctuation in  $\xi$  can be associated to the existence of  $\frac{C}{T}$ QPT at the critical point during the melting or solidification process in such a way that if we continue extracting heat from the LiCl system, then one has the liquid to solid transformation due to  $[\xi^{\text{liquid}} \rightarrow \xi^{\text{solid}}] > [\xi^{\text{liquid}} \leftarrow \xi^{\text{solid}}]$  that freezes LiCl completely. The formation of bonds (or releasing of heat) during solidification occur continuously with respect to time that involves complete modification of the time-dependent many-body wave function ( $\Psi(t)$ ). Within IET formalism, we do not require to know the changes in  $\Psi(t)$ , instead, we have  $\xi(t)$  as the fundamental interaction-strength functional, which changes continuously and originates from the chemical constituents of a system. In our earlier work [6], we have renormalized  $C_v$  that can be exploited here to rewrite Eq. (3.15) for  $T = T_\theta$

$$(3.16) \quad d\tilde{S}_{\text{eq}}^{\text{non}}(t) = \frac{\tilde{C}_v(t)_{\text{eq}}^{\text{non}}}{T_\theta} dt = \frac{C_v(T)}{T_\theta} \exp \left[ -\frac{3}{2} \lambda \xi(t) \right] dt,$$



which reinforces the logic that any change to the interaction strength during solidification, even though  $T$ -independent at the critical point, never ceases to be  $t$ -dependent, giving rise to  $S_{\text{liquid}} \rightarrow S_{\text{solid}}$  and  $C_v^{\text{liquid}} \rightarrow C_v^{\text{solid}}$  transitions. These  $t$ -dependent transitions,  $\tilde{S}_{\text{eq}}^{\text{non}}(t)$  and  $\tilde{C}_v(t)_{\text{eq}}^{\text{non}}$  can be readily captured via  $\xi(t)$  without any divergence. In addition to that, we now claim that the solid  $\rightleftharpoons$  liquid transitions at  $T = T_\theta$  are associated to  ${}^C_T$ QPT. An essential point to note here is that we did not identify  $C_v(T)$  in Eq. (3.16) as the nonequilibrium specific heat at the critical point because  $C_v(T)$  reduces to  $C_v^{\text{liquid}}(T)$  during solidification, whereas,  $C_v(T) \rightarrow C_v^{\text{solid}}(T)$  during melting. We also remind the readers to take note here that unlike  $S_\xi$  and  $S_{\text{D}}$ ,  $\{\tilde{S}, S\} \in \mathbb{R}^+$  because  $\{N/q, N_{\text{D}}/q_{\text{D}}\} \in (0, 1]$ . To those who are not comfortable with  $\{S_\xi, S_{\text{D}}\} \in \mathbb{R}^-$ , we define an alternative equation

$$(3.17) \quad S_\xi(+) = k_{\text{B}} \ln \left\{ \frac{q}{\exp[\mu + \lambda(E_0 \pm \xi)] + 1} \right\} = k_{\text{B}} \ln N,$$

which can be obtained from Eq. (3.8) and recall here that  $N$  is the number of excited electrons. Similarly,

$$(3.18) \quad S_{\text{D}}(+) = k_{\text{B}} \ln \left\{ \frac{q_{\text{D}}}{\exp[\lambda_{\text{B}} E e^{(1/2)\lambda\xi}] - 1} \right\} = k_{\text{B}} \ln N_{\text{D}},$$

in this case,  $N_{\text{D}}$  is the number of ions being displaced (or excited) from their crystallographic sites. Apart from Eqs. (3.17) and (3.18), we can also enforce positivity by rewriting Eq. (3.8) such that

$$(3.19) \quad S_\xi^+ = -k_{\text{B}} \frac{N}{q} \ln \frac{N}{q} \quad \text{and} \quad S_{\text{D}}^+ = -k_{\text{B}} \frac{N_{\text{D}}}{q_{\text{D}}} \ln \frac{N_{\text{D}}}{q_{\text{D}}},$$

because if  $N_1/q > N_2/q$  and  $0 \leq N_{1,2}/q \leq 1$ , then

$$(3.20) \quad -\frac{N_1}{q} \ln \frac{N_1}{q} > -\frac{N_2}{q} \ln \frac{N_2}{q},$$

which will guarantee  $S_1 \geq 0$ ,  $S_2 \geq 0$  and  $S_1 > S_2$  because  $N/q$  increases or decreases faster than  $\ln(N/q)$ . For example, taking  $N = 1$ ,  $q = x$ ,  $f(x) = 1/x$  and  $g(x) = \ln(1/x)$ , one can write  $h[f, g] = (1/x) \ln(1/x)$ , subsequently it is straightforward to show  $d^m f/dx^m > d^m g/dx^m$  is always true when  $x \geq 1$  and  $m \geq 1$  where  $x \in \mathbb{R}^+$  and  $m \in \mathbb{N}^*$ . In addition,  $S_1 > S_2$  is consistent with increasing entropy if  $N/q$  gets larger, and consequently we will always have  $\{S_\xi(+), S_\xi^+, S_{\text{D}}(+), S_{\text{D}}^+\} \in \mathbb{R}^+$  where  $\mathbb{R}^+$  and  $\mathbb{N}^*$  are the set of real positive numbers and positive integers, including zero, respectively.

In summary, any first-order TPT has got to go through a  ${}^C_T$ QPT at constant  $T$  such that

$$(3.21) \quad \lim_{\hbar \rightarrow 0} {}^C_T \text{QPT} = \text{TPT} \quad \text{and} \quad {}^C_T \text{QPT} \supset \text{TPT},$$

which means, any first-order TPT is a limiting case in the absence of quantum fluctuations, and therefore  ${}^C_T$ QPT is a proper superset of TPT. These two claims are strong, thus we will need to provide logical proofs. The proofs consist of two parts that correspond to two claims. The first one is given above when we discussed the solidification phenomenon for LiCl, establishing the correctness of Statement 1.

**Statement 1:** All first-order TPT must go through a thermal-assisted  ${}^C$ QPT at constant  $T$ .

The second proof proves Eq. (3.21), which will be exposed shortly.

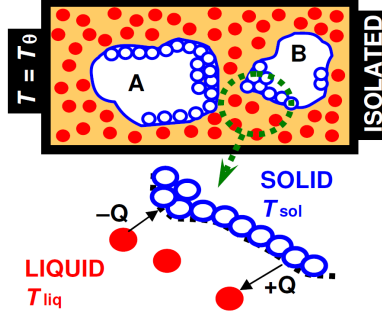


FIGURE 2. Both atomic Li and Cl in the liquid phase are denoted with filled red circles, while the blue circles represent the ionic Li and Cl in the solid phase. The two blue islands labeled A and B are solid particles, immersed in the liquid-phase. This system has been deliberately isolated at the critical point when  $T = T_\theta = 610^\circ\text{C}$  such that the solid phase coexists indefinitely within the liquid phase. The magnified sketch beneath the main diagram shows the temperature differences between the solid phase ( $T_{\text{sol}}$ ) and its surrounding liquid phase ( $T_{\text{liq}}$ ) such that  $T_{\text{liq}} > T_\theta > T_{\text{sol}}$  and  $T_{\text{liq}} - T_{\text{sol}} \ll T_\theta$ . At the boundary, the system is in extreme nonequilibrium where Li or Cl from the liquid phase may react to form a rigid ionic bond, and release heat ( $-Q$ ) as energy. Conversely, the same amount of heat is absorbed ( $+Q$ ) by Li or Cl in the solid phase so as to break free from the solid to liquid phase.

#### 4. CONTINUOUS FINITE-TEMPERATURE QUANTUM PHASE TRANSITION

Thus far, we have exposed the existence of  $^C_T$ QPT during LiCl solidification at  $T = T_\theta$  (see the vertical arrow in the inset of Fig. 1), which is commonly accepted as a first-order TPT without going into the details of  $^C_T$ QPT. Proving Eq. (3.21) requires one to track  $^C_T$ QPT or the changes in  $\xi(t)$  during solidification for constant  $T = T_\theta$ . Alternatively, one may also prove Eq. (3.21) by tracking the horizontal arrow pointing left shown in the inset of Fig. 1 by systematically changing the chemical composition via substitutional doping of Cl with Br and followed by I such that  $\text{LiCl} \rightarrow \text{LiBr} \rightarrow \text{LiI}$  at constant  $T = 552^\circ\text{C}$ , which is the melting point of LiBr. We will first address the  $^C_T$ QPT occurring during solidification (for constant  $T = 610^\circ\text{C}$ ).

The above  $^C_T$ QPT during solidification of LiCl system can be captured by isolating the system right at the critical point ( $T_\theta = 610^\circ\text{C}$ ) as shown schematically in Fig. 2. Here, the liquid phase Li and Cl are indicated with filled red circles, while the same elements in the solid phase are drawn as blue circles, but we did not bother to completely fill the solid phase with blue circles. Relevant nonequilibrium processes occur at the boundary between these two phases. These processes are due to chemical reactions between the highly-polarized Li (small  $\xi_{\text{Li}}$ ) and the least-polarized Cl (large  $\xi_{\text{Cl}}$ ) giving rise to the chemical association between them, forming the solid phase, which releases energy as heat ( $-Q$ ) into the liquid phase. This energy transfer increases the kinetic energy of the liquid-phase Li and Cl that

will eventually collide onto the solid-particle surfaces with increasing frequency, and thus could transfer this energy ( $+Q$ ) back into the solid phase to initiate chemical dissociation of LiCl solid. These two thermal-assisted processes (due to  $\pm Q$ ) are the causes for this thermal-assisted (or finite-temperature)  $^C$ QPT. In a macroscopic point of view, this particular isolated system, containing both solid and liquid phases, is in equilibrium because the average rate of melting and solidification is the same, hence the solid-to-liquid and liquid-to-solid transitions ( $^C_T$ QPT) are in balance. But we need to go deeper to track the physico-chemical processes at the solid|liquid interface, which can be done with IET. For instance, the energy level spacings in the liquid and solid phases are  $\xi_{\text{liquid}}^{\text{LiCl}}$  and  $\xi_{\text{solid}}^{\text{LiCl}}$ , respectively, and since the valence electrons in the liquid phase are all in the excited states (thermally polarized) then this implies  $\xi_{\text{liquid}}^{\text{LiCl}} < \xi_{\text{solid}}^{\text{LiCl}}$ . This inequality is strictly valid because the excited energy-level spacings are always narrower due to weak electron-electron ( $e-e$ ) interaction in the presence of weak electron-nucleus ( $e\text{-nuc}$ ) attraction. Conversely, large energy level spacings are inevitable for the energy levels close to the nucleus [5].

Substituting  $\xi_{\text{liquid}}^{\text{LiCl}} < \xi_{\text{solid}}^{\text{LiCl}}$  into Eq. (3.19) leads to  $\text{liq}S_{\xi}^+ > \text{sol}S_{\xi}^+$  and  $\text{liq}S_{\text{D}}^+ > \text{sol}S_{\text{D}}^+$ , which then allow one to correctly conclude  $S_{\text{liquid}} > S_{\text{solid}}$  where  $S_{\text{liquid}} = \text{liq}S_{\xi}^+ + \text{liq}S_{\text{D}}^+$  and  $S_{\text{solid}} = \text{sol}S_{\xi}^+ + \text{sol}S_{\text{D}}^+$ . However, as we have noted earlier,  $S_{\text{solid}} < S_{\text{eq}}^{\text{non}} < S_{\text{liquid}}$  is invalid because we need to take the nonequilibrium effect into account. We now know that this effect occurs maximally at the critical point (when  $T = T_{\theta}$ ), and at the solid|liquid interface where  $S_{\text{eq}}^{\text{non}} = S_{\text{liquid}} + S_{\text{solid}} + S_{\text{face}}^{\text{inter}}$ , and therefore  $S_{\text{solid}} < S_{\text{liquid}} < S_{\text{eq}}^{\text{non}}$  that guarantees the existence of a first-order TPT, while  $S_{\text{face}}^{\text{inter}}$  on the other hand, ensures the existence of a  $^C_T$ QPT, as well as the coexistence of both solid and liquid phases (see Fig. 2). This means that if  $S_{\text{face}}^{\text{inter}} = 0$ , then  $T \neq T_{\theta}$  and consequently we have  $S_{\text{eq}}^{\text{non}} \rightarrow S_{\text{liquid}}$  for  $T > T_{\theta}$  or  $S_{\text{eq}}^{\text{non}} \rightarrow S_{\text{solid}}$  for  $T < T_{\theta}$ . Using Eq. (3.16), the non-divergent and renormalized

$$(4.1) \quad \tilde{C}_v(T_{\theta}, t)_{\text{eq}}^{\text{non}} = C_v(T) \exp \left\{ -\frac{3}{2} \lambda \left[ \sum_j J_j \xi_{\text{solid}} + (1 - J_j) \xi_{\text{liquid}} \right] \right\},$$

in which, we have defined  $\xi(t) = \sum_j J_j \xi_{\text{solid}} + (1 - J_j) \xi_{\text{liquid}}$  where  $j = \{t_1, t_2, \dots, t_n\}$ ,  $J = \mathbf{x}_{\text{solid}}^{\text{LiCl}} / \mathbf{x}_{\text{total}}^{\text{LiCl}}$  and  $J \in [0, 1]$ . Here,  $\mathbf{x}_{\text{solid}}^{\text{LiCl}}$  is the number of Li and Cl atoms in the solid phase only, and  $\mathbf{x}_{\text{total}}^{\text{LiCl}}$  is the total number of Li and Cl atoms in both liquid and solid phases (or in a given system). Moreover,  $J$  does not necessarily increase with time, if the heat-exchange fluctuates ( $\pm Q$ ), and the total time between  $t_1$  and  $t_n$  is the time taken for a complete solidification of liquid LiCl for constant  $T = T_{\theta}$ . Equation (4.1) strictly implies that the magnitude of  $\tilde{C}_v(t)_{\text{eq}}^{\text{non}}$  does not change with  $T$  only, but also with respect to changes in the interaction-strength parameter,  $\xi(t)$ . In particular,  $\tilde{C}_v(t)_{\text{eq}}^{\text{non}}$  can change due to changes in  $\xi(t)$  from  $\xi_{\text{liquid}}$  to  $\xi_{\text{solid}}$  during solidification of LiCl liquid. In this latter case, the heat-exchange as depicted in Fig. 2 is solely used to change the interaction strength via  $\xi_{\text{solid}} \rightleftharpoons \xi_{\text{liquid}}$ .

If one employs an unrenormalized specific-heat equation, then it is always divergent for  $T = T_{\theta}$  because it is undefined at this critical point. On the other hand, Eq. (4.1) is well-defined such that  $\xi$  can be exploited at the critical points, without any divergence. For example,  $\xi_{\text{liquid}}$  and  $\xi_{\text{solid}}$  are constants for  $T > T_{\theta}$  and  $T < T_{\theta}$ , respectively, and any heat exchanges that may exist between a given system and its surrounding only decrease or increase the system's temperature. At

the critical point however, the heat exchanges are used only to modify the system's physico-chemical properties, hence, the system's temperature remains constant. In other words, the renormalized specific-heat equation (Eq. (4.1)) reduces to

$$(4.2) \quad \tilde{C}_v^{\text{liquid}}(T) = C_v^{\text{liquid}}(T) \exp \left[ -\frac{3}{2} \lambda \xi_{\text{liquid}} \right],$$

for liquid LiCl ( $T > T_\theta$ ), and for solid LiCl ( $T < T_\theta$ ), one just need to switch the label "liquid" with "solid" in the equation above. However, neither of these equations can be applied when  $T = T_\theta$ . We need Eq. (4.1) for  $T = T_\theta$ . This completes the proof for Statement 1.

If we now follow the horizontal arrow given in the inset of Fig. 2, we can show that both transitions (for vertical and horizontal arrows) are thermal-assisted  $^C_T$ QPT, one occurring during solidification (discussed above for the vertical arrow) and the other originates due to changing chemical composition (at a constant temperature). For example, the first  $^C_T$ QPT at the critical point during solidification (constant  $T = T_\theta$ ) is initiated by the heat-exchange between the liquid and solid LiCl, where  $dS = \delta Q/T_\theta$ , and from Eq. (3.9),

$$(4.3) \quad d|S_\xi| = dS = \frac{\delta Q}{T_\theta} = \left| -\frac{(E_0 \pm d\xi) + E_F^0}{T_\theta} \right|, \quad |S_\xi| \in \mathbb{R}^+.$$

Equation (4.3) correctly implies: (a) increasing absorption of heat in a system increases the entropy of that system, or vice versa, (b) any amount of change in  $Q$  ( $\delta Q$ ) or  $\xi$  ( $d\xi$ ) corresponds accordingly to a change in entropy, as it should be, however, (c) the entropy of a given system decreases if  $\xi$  increases, as strictly required by Eq. (3.9), (d) systems with large  $\xi$  need large amount of heat to initiate changes such as melting, for example, from Table 2, we know  $[\xi_{\text{Br}} < \xi_{\text{Cl}}] \rightarrow [\xi_{\text{LiBr}} < \xi_{\text{LiCl}}]$  and therefore  $T_\theta^{\text{LiBr}} < T_\theta^{\text{LiCl}}$ , and (e) large amount of heat is required to be removed or added to initiate large changes to  $\xi$ , for example  $\xi_{\text{liquid}}^{\text{LiCl}} \rightleftharpoons \xi_{\text{solid}}^{\text{LiCl}}$ . Here,  $\xi_{\text{liquid}}^{\text{LiCl}}$  is a constant, while  $Q$  is the amount of heat removed to initiate the change,  $\xi_{\text{liquid}}^{\text{LiCl}} - Q \rightarrow \xi_{\text{solid}}^{\text{LiCl}}$ . Therefore, (d) refers to the entropy-change of a system prior to any phase transition, *i.e.*, for constant  $\xi$  and  $T < T_\theta$  or  $T > T_\theta$ , in contrast, (e) reveals the changes in the intrinsic physico-chemical properties of a system due to changing  $\xi$  when  $T = T_\theta$ . This means that  $d|S_\xi|$  is only valid at the critical point, or when  $T = T_\theta$  because  $\xi$  does not change with  $T$ , but it changes significantly when the physico-chemical properties of a given system change.

In order to understand the existence of thermal-assisted  $^C$ QPT due to doping (follow the horizontal arrow in the inset of Fig. 2), we increase Br content, replacing Cl for constant  $T$  to obtain a system defined by  $\text{LiCl}_{1-a_1}\text{Br}_{a_1}$ . The inequality,  $\xi_{\text{Br}} < \xi_{\text{Cl}}$  implies  $\xi$  decreases with increasing Br content where this doping is carried out for constant  $T = 552^\circ\text{C}$ . Now, the critical point can be obtained for  $a_1 = 1$ , and at this point,  $T = T_\theta = 552^\circ\text{C}$ , which is the melting point of LiBr. As a consequence, if  $\xi_{\text{solid}}^{\text{LiCl}} \rightarrow \xi_{\text{solid}}^{\text{LiBr}}$  is achieved through doping at  $T = T_\theta^{\text{LiBr}}$ , then  $Q$  activates the melting process, such that  $\xi_{\text{solid}}^{\text{LiBr}} + Q \rightarrow \xi_{\text{liquid}}^{\text{LiBr}}$ . However, we point out that  $Q = \xi_{\text{liquid}}^{\text{LiBr}} - \xi_{\text{solid}}^{\text{LiBr}}$  is false. Note here that the above stated doping-induced  $^C_T$ QPT can occur for any constant temperature, and even for  $T = 0\text{K}$ . For instance, electronic phase transition (metal-to-insulator) due to doping can occur in doped-cuprates at zero Kelvin, giving rise to the usual continuous quantum phase transition ( $_{0\text{K}}$ QPT), as explained by Sachdev [23]. Nevertheless, Eq. (3.21)

remains true for both  $\frac{C}{T}$ QPT and  ${}_{0K}$ QPT, in accordance with the proof given for the horizontal arrow of Fig. 1.

In summary, the so-called activation energy in this chemical association should be equal to  $Q$ , which is required to complete the liquid-to-solid transition, or vice versa. In other words, to complete the  $\xi_{\text{liquid}}^{\text{LiCl}} \rightarrow \xi_{\text{solid}}^{\text{LiCl}}$  or  $\xi_{\text{solid}}^{\text{LiBr}} \rightarrow \xi_{\text{liquid}}^{\text{LiBr}}$  transformation, significant changes to the  $t$ -dependent many-body wave function are necessary, for example,  $\Psi(t)_{\text{liquid}}^{\text{LiCl}} \rightarrow \Psi(t)_{\text{solid}}^{\text{LiCl}}$ . The existence of such a transformation in  $\Psi(t)$  has been proven within a new quantum adiabatic theorem developed for chemical reactions [30], which can be used to understand why the wave function of unreacted species need to be combined linearly or written in a different form for the compounds formed after the chemical associations. Interestingly, Müller and Goddard [31] have also pointed out such a case must exist during chemical associations. Thus far, we have exploited the formalism developed for IET such that the only *a priori* information one required to know is the atomic energy-level spacings listed in Table 2.

## 5. CONCLUSIONS

We first entered into the realm of thermodynamics and statistical mechanics to show that all thermal phase transitions occurring in any matter is a proper subset of quantum phase transition, even though at times, it is convenient to ignore the quantum effects, for example during the transition from a solid to liquid phase. We went on to renormalize the entropy and the Bose-Einstein statistics solely to prove the existence of the non-divergent specific heat capacity at the critical point via the energy level spacing renormalization method. At the critical point, the thermal energy is used to change the energy-level spacing of a system, which in turn changes the physico-chemical properties of that system. Those properties are of course different if the system is in solid phase, compared to liquid. The critical points we chose to investigate were the melting points of single-valent ionic bonded salts. Here, we have formally shown that the finite-temperature continuous quantum phase transition ( $\frac{C}{T}$ QPT) is responsible for the thermal phase transition during melting and solidification processes, as well as during substitutional doping at a constant temperature. In other words,  $\frac{C}{T}$ QPT is a thermal-assisted continuous quantum phase transition.

## ACKNOWLEDGMENTS

This work was supported by Sebastiammal Innasimuthu, Arulsamy Innasimuthu and Arokia Das Anthony. I thank Naresh Kumar Mani for his kind hospitality during my short stay in Cachan, France. I am grateful to several anonymous referees from the Pramana Journal of Physics, Journal of Physics and Chemistry of Solids and Physica Status Solidi B for correctly pointing out that IET is also related to the Green function and the renormalization group theory. Special thanks to an anonymous reader for sending some interesting historical facts surrounding the second law of thermodynamics.

## REFERENCES

- [1] S. Sachdev, *Quantum Phase Transitions* (2004) ([qpt.physics.harvard.edu/c40.pdf](http://qpt.physics.harvard.edu/c40.pdf)).
- [2] A. D. Arulsamy, Z. Kregar, K. Eleršič, M. Modic, U. S. Subramani, Phys. Chem. Chem. Phys. **13**, 15175 (2011).

- [3] A. D. Arulsamy, *Physica C* **356**, 62 (2001).
- [4] A. D. Arulsamy, *Phys. Lett. A* **334**, 413 (2005).
- [5] A. D. Arulsamy, *Pramana J. Phys.* **74**, 615 (2010); A. D. Arulsamy, PhD thesis, The University of Sydney, Australia (2009).
- [6] A. D. Arulsamy, *Ann. Phys. (N.Y.)* **326**, 541 (2011).
- [7] A. D. Arulsamy, X. Y. Cui, C. Stampfl, K. Ratnavelu, *Phys. Status Solidi B* **246**, 1060 (2009).
- [8] A. D. Arulsamy, *Phys. Lett. A* **300**, 691 (2002).
- [9] A. D. Arulsamy, K. Ostrikov, *J. Supercond. Nov. Magn.* **22**, 785 (2009).
- [10] A. D. Arulsamy, U. Cvelbar, M. Mozetic, K. Ostrikov, *Nanoscale* **2**, 728 (2010).
- [11] A. D. Arulsamy, K. Eleršič, M. Modic, U. Cvelbar, M. Mozetič, *ChemPhysChem* **11**, 3704 (2010).
- [12] J. Simon, W. S. Bakr, R. Ma, M. E. Tai, P. M. Preiss, M. Greiner, *Nature* **472**, 307 (2011).
- [13] S. Sachdev, B. Keimer, *Phys. Today* **64**, 29 (2011).
- [14] T. Senthil, *Phys. Rev. B* **78**, 035103 (2008).
- [15] S. Burdin, D. R. Grempel, A. Georges, *Phys. Rev. B* **66**, 045111 (2002).
- [16] T. Senthil, M. Vojta, S. Sachdev, *Phys. Rev. B* **69**, 035111 (2004).
- [17] T. Senthil, M. Vojta, S. Sachdev, *Physica B* **359-361**, 9 (2005).
- [18] D. J. Scalapino, *Physica C* **470**, S1 (2010).
- [19] P. Mohan, R. Narayanan, T. Vojta, *Phys. Rev. B* **81**, 144407 (2010).
- [20] P. Mohan, P. M. Goldbart, R. Narayanan, J. Toner, T. Vojta, *Phys. Rev. Lett.* **105**, 085301 (2010).
- [21] T. Senthil, *Ann. Phys. (N.Y.)* **321**, 1669 (2006).
- [22] S. Sachdev, T. Senthil, *Ann. Phys. (N.Y.)* **251**, 76 (1996).
- [23] S. Sachdev, *Phys. Status Solidi B* **247**, 537 (2010).
- [24] S. Sachdev, X. Yin, *Ann. Phys. (N.Y.)* **325**, 2 (2010).
- [25] T. Senthil, R. Shankar, *Phys. Rev. Lett.* **102**, 046406 (2009).
- [26] D. R. Lide, *CRC Handbook of Chemistry and Physics*, (CRC Press, 84th edition, 2004, USA).
- [27] M. J. Winter, ([www.webelements.com](http://www.webelements.com)). The Elements Periodic Table: Essential Data and Description.
- [28] D. J. Griffiths, *Introduction to Quantum Mechanics*, Second edition (Prentice-Hall, New Jersey, 2005, USA).
- [29] H. E. Stanley, *Introduction to Phase Transitions and Critical Phenomena*, (Oxford University Press, N.Y., 1971, USA).
- [30] A. D. Arulsamy, *Prog. Theor. Phys. (Kyoto)* Accepted (2011).
- [31] R. P. Müller, W. A. Goddard, *Valence Bond Theory*, Reprinted from the Encyclopedia of Physical Science and Technology, Academic Press (2002).

*E-mail address:* [sadwerdna@gmail.com](mailto:sadwerdna@gmail.com)

CONDENSED MATTER GROUP, DIVISION OF INTERDISCIPLINARY SCIENCE, 79-F-02-08 KETUMBAR HILL, JALAN KETUMBAR, 56100 KUALA-LUMPUR, MALAYSIA